Mendeleev Communications

Mendeleev Commun., 2027, **37**, in press

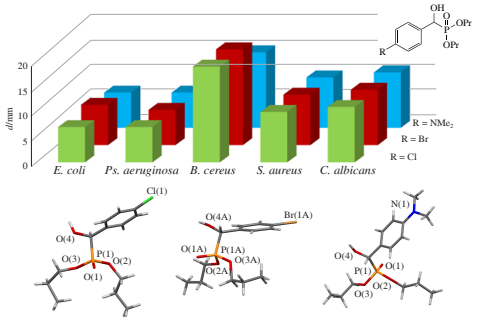
Molecular structure, thermal, and antimicrobial properties of dipropyl [hydroxy(aryl)methyl]phosphonates

Rustam R. Davletshin,*[a] Andrey N. Sedov,[a] Kamil A. Ivshin,[b] Marina P. Shulaeva,[c] Alexander V. Gerasimov,[a] Natal'ya V. Davletshina,[a] Timofey T. Senchenko[a] and Polina A. Kuryntseva[d]

[a] *A. M. Butlerov Institute of Chemistry, Kazan Federal University, 420008 Kazan, Russian Federation. E-mail: alchemy-rus@yandex.ru*
[b] *A. E. Arbuzov Institute of Organic and Physical Chemistry, FRC Kazan Scientific Center of the Russian Academy of Sciences, 420088 Kazan, Russian Federation*
[c] *Kazan State Medical Academy, 420012 Kazan, Russian Federation*
[d] *Institute of Environmental Sciences, Kazan Federal University, 420008 Kazan, Russian Federation*

DOI: 10.71267/mencom.8102

The molecular structures, thermal decomposition behavior, and antimicrobial activity of dipropyl α-hydroxy(aryl)-methylphosphonates were investigated. It was shown that the nature of the *para*-substituent dictated the crystal packing *via* a hierarchy of secondary interactions, whereas thermal degradation correlated with the nature of the substituent on the benzene ring. All compounds exhibited antimicrobial activity against *B. cereus* and *S. aureus* comparable to that of benzalkonium chloride, as well as activity against *Candida* fungi.



Keywords: α-hydroxyphosphonates, Abramov reaction, molecular structure, thermal stability, antimicrobial activity.

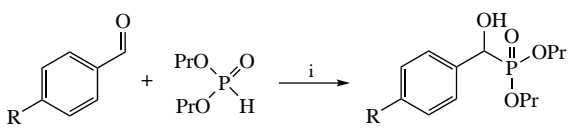
Among organophosphorus compounds, α-hydroxyalkyl-phosphonates are recognized for their good chemical stability and favorable bioavailability. In recent years, they have attracted growing research interest due to their antimicrobial, antioxidant, herbicidal, anticancer, anti-HIV, and anti-inflammatory properties.[1–6] Their ability to suppress the growth of bacteria, fungi, and viruses stems mainly from the inhibition of essential microbial enzymes or interference with metabolic and structural pathways.[7–12] Consequently, α-hydroxyphosphonates are considered promising scaffolds for the development of new antibiotics, especially in the context of increasing resistance to conventional drugs.[13–18] The simultaneous presence of a phosphonate moiety and an α-hydroxyl group allows these compounds to interact with key metabolic enzymes and cellular membranes, thereby disrupting the metabolism of pathogenic cells.[19–27]

X-ray structures of numerous α-hydroxyphosphonate derivatives were reported.[28–30] It was shown that the presence of a tertiary α-carbon atom or a sterically and electronically shielded α-CH proton favored dimer formation.[31] Additionally, the type and degree of crowding of *ortho*-substituents on the aromatic ring determined whether chains or dimers were formed.

In our previous work, we investigated the structure, properties, and biological activity of α-bromocinnamaldehyde derivatives.[32] The present study follows this research by focusing on phosphonate derivatives. Detailed knowledge of the regularities that govern the association of molecules in the solid state and lead to the formation of ordered crystalline architectures provides valuable information on molecular geometry, intermolecular contacts, and electronic characteristics. Simultaneous investigation of crystal structure and antimicrobial properties is important not only for establishing structure–activity relationships but also for practical applications. These include the development of solid dosage forms, bioavailability assessment (considering solubility and polymorphism), as well as storage stability and analytical identification.

α-Hydroxy(aryl)methylphosphonates **1–3** were chosen for the studies. Of note, short alkyl chain (namely, *n*-propyl) esters was envisioned to impart sufficient water solubility of the target molecules, and hence enable antimicrobial testing in aqueous media. Target products **1–3** were obtained *via* the Abramov reaction from the corresponding aldehydes (Scheme 1).[32–35] The transformation was completed within 0.5 h under solvent-free conditions affording α-hydroxymethylphosphonates **1–3** in excellent yields.

The molecular structures of all compounds were confirmed by a combination of spectroscopic methods and single-crystal X-ray diffraction (Figure 1, see also Online Supplementary Materials).† Reasonably, ^{1}H and ^{13}C NMR spectra showed non-equivalency of the two propoxy groups. Characteristic



1 R = Cl, 92%
2 R = Br, 95%
3 R = NMe_2, 90%

Scheme 1 *Reagents and conditions*: i, K_3PO_4 (10 mol%), solvent free, room temperature, 30 min.

© 2027 Mendeleev Communications

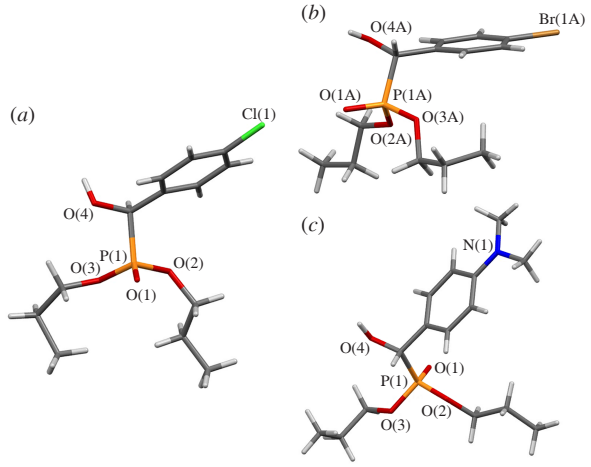


Figure 1 Molecular structures of compounds (*a*) **1**, (*b*) **2**, and (*c*) **3**.

signals included the P–CH proton as a doublet at ~4.9 ppm and the P–CH carbon as a doublet at ~70 ppm ($^1J_{P-C} \approx 160$ Hz). The OH proton was observed only for compound **1** (~4.3 ppm), whereas for **2** and **3** it was absent due to fast exchange. Characteristic $\nu_{(=C-H)}$ and $\nu_{(C=C)}$ bands in the FTIR spectra were in accordance with literature data.[36] Of special importance were broad $\nu_{(OH)}$ band at 3100–3300 cm^{-1} as well as $\nu_{(P=O)}$ band diminished and downshifted to ~1206–1230 cm^{-1}, that evidenced about intermolecular O–H···O=P hydrogen bonding. This H-bonding was also confirmed by the X-ray diffraction analysis.

For compounds **1** and **3** (in contrast to bromine-substituted derivative **2**), the dominant supramolecular motif was a one-dimensional chain formed by classical O–H···O hydrogen bonds (Table S2). Despite this common feature, the three-dimensional packing differed markedly depending on the *para*-substituent. The chlorine derivative crystallized in the orthorhombic space group *Pbca* with one molecule in the asymmetric part. Molecules of the same chirality were linked into chains along the 2_1 screw axis (parallel to the *b*-axis). These chains were connected by non-classical C–H···O hydrogen bonds and Cl···H contacts to form columns, which were further stabilized by H···H interactions, while the chlorine atoms were oriented toward the hydrophobic region (see Figure S2).

In contrast, replacing chlorine with bromine substantially altered the intermolecular interactions and crystal packing. Compound **2** crystallized in the monoclinic space group *C*2/*c* with four crystallographically independent molecules forming two hydrogen-bonded dimers. These dimers were reinforced by C–H···O contacts and linked through type-I Br···Br halogen interactions into dimeric chains. The chains further assembled into columns *via* Br···H, C–H···O, and C–H···π interactions (see Figure S3). Notably, Br···Br contacts are unique to the propyl esters derivative and are absent in the corresponding ethyl and isopropyl analogues.[37,38]

Introduction of the bulky dimethylamino group in compound **3** resulted in crystallization of an enantiomerically pure *S*-isomer. As in compound **1**, the primary packing motif consisted of O–H···O hydrogen-bonded chains. A second, perpendicular chain system was generated by C–H···O interactions between a methyl group of the NMe_2 substituent and the phosphoryl oxygen atom; propagating along the *b* and *c* axes (see Figure S4). The observed competition between chain-linked and dimeric supramolecular motifs in compounds **1**–**3** is consistent with literature data on α-aryl-α-hydroxyphosphonates, where the packing mode was governed by the nature and steric demand of substituents.[7,11]

Thermal stability is an important parameter for compounds with potential antimicrobial applications, as it influences their handling, storage, and formulation. The DSC curves of all synthesized phosphonates **1**–**3** exhibited distinct endothermic melting peaks (see Online Supplementary Materials). No significant mass loss occurs below 150 °C, indicating the absence of volatile impurities or residual solvents (*e.g.*, water). Above this temperature, mass loss corresponds to thermal decomposition. Table 1 provides details on the thermal stability of compounds **1**–**3**, including the initial degradation temperature (T_{onset}), maximum degradation temperature (T_{max}) and mass loss [Δm (%)].

Under an argon atmosphere, all three compounds begin to decompose in the temperature range 173–201 °C. The onset of decomposition is attributed to the cleavage of the propyl group from the phosphorus atom, which is consistent with the known lower thermal stability of the P–O–C bond at lower temperatures compared to other bonds in the molecule.[39–41]

For the halogenated derivatives **1** and **2**, a single complex decomposition peak is observed in the range 174–276 °C, with a total mass loss of 65–69% (see Online Supplementary Materials). This behaviour was attributed to the simultaneous cleavage of

Table 1 TG-DSC data for products **1**–**3**.

Compound	mp/°C	T_{onset}/°C		T_{max}/°C		Loss of mass Δm (%) (ΔT/°C)	
		O–Pr	P–C–C_{arom}	O–Pr	P–C–C_{arom}	O–Pr	P–C–C_{arom}
1	53.9	174		235.3 and 251.6		64.5 (174–257)	
2	71.9	188		238.4 and 257.6		69.3 (188–276)	
3	88.6	133	263	186.8	289.4	27.4 (133–263)	26.9 (263–400)

† *Crystal data for* **1**. $C_{13}H_{20}ClO_4P$ (M = 306.71 g mol^{-1}), orthorhombic, space group *Pbca* at 273(2) K: a = 15.689(3), b = 8.3013(14) and c = 24.902(5) Å, V = 3243.3(10) Å^3, d_{calc} = 1.256 g cm^{-3}, μ(MoKα) = 0.340 mm^{-1}, F(000) = 1296. A total of 58837 reflections were collected (3157 independent reflections and 1937 observed reflections, R_{int} = 0.1243), GOOF 1.084, final R indices [$I > 2\sigma(I)$]: R_1 = 0.1058, wR_2 = 0.2525, R indices (all data): R_1 = 0.1625, wR_2 = 0.3054.

Crystal data for **2**. $C_{13}H_{20}BrO_4P$ (M = 351.17 g mol^{-1}), monoclinic, space group *C*2/*c* at 100(2) K: a = 44.950(5), b = 10.3162(11) and c = 33.069(3) Å, β = 124.806(3)°, V = 12591(2) Å^3, d_{calc} = 1.478 g cm^{-3}, μ(MoKα) = 2.720 mm^{-1}, F(000) = 5728. A total of 286259 reflections were collected (12342 independent reflections and 7856 observed reflections, R_{int} = 0.1597), GOOF 1.054, final R indices [$I > 2\sigma(I)$]: R_1 = 0.0624, wR_2 = 0.1443, R indices (all data): R_1 = 0.1125, wR_2 = 0.1764.

Crystal data for **3**. $C_{15}H_{26}NO_4P$ (M = 315.34 g mol^{-1}), monoclinic, space group $P2_1$ at 100(2) K: a = 10.3689(10), b = 7.8755(8) and c = 10.9165(11) Å, β = 114.021(3)°, V = 814.24(14) Å^3, d_{calc} = 1.286 g cm^{-3}, μ(MoKα) = 0.184 mm^{-1}, F(000) = 340. A total of 15955 reflections were collected (4152 independent reflections and 3531 observed reflections, R_{int} = 0.0674), GOOF 1.068, final R indices [$I > 2\sigma(I)$]: R_1 = 0.0561, wR_2 = 0.0993, R indices (all data): R_1 = 0.0739, wR_2 = 0.1083.

CCDC 2503858, 2503859 and 2503856 contain the supplementary crystallographic data for this paper. These data can be obtained free of charge from The Cambridge Crystallographic Data Centre *via* https://www.ccdc.cam.ac.uk.

both propyl group and the P–C–C(aromatic) bond.[28,40] The electron-withdrawing nature of chlorine and bromine reduces the electron density in the benzene ring, weakening the C–C bond at the *ipso* position and thereby facilitating the simultaneous elimination of the propyl and aromatic fragments.

Compound **3** showed the most pronounced stepwise decomposition. An initial mass loss of 13.7% occurred at an onset temperature of 133 °C, corresponding to the elimination of one propyl group. A second mass loss at higher temperature (up to 208 °C) was assigned to the loss of the second propyl group. The P–C–C(aromatic) bond cleaved only above 263 °C, with a total mass loss of 26.9% by 400 °C. Interestingly, decomposition was not complete at 400 °C. We hypothesized that the loss of the first propyl group resulted in the formation of the phosphonic monoester that can form a stabilizing hydrogen bond with a dimethylamino group (*e.g.*, $Me_2N\cdots H–O–P$), thus reducing the degradation rate. This hypothesis was supported by an exothermic event in the DSC curve, indicating a thermodynamically favorable process with energy release.

The *in vitro* antimicrobial activity of α-hydroxyphosphonates **1**–**3** was assessed against a panel of opportunistic pathogens using the agar well diffusion method. The growth inhibition zones were measured to evaluate both bactericidal and fungicidal effects. All tests were carried out using 1% ethanol solutions, and the results are summarized in Table 2. Ethanol alone produced no inhibition zones.

All tested compounds were practically inactive against the gram-negative bacteria *E. coli* and *P. aeruginosa*. Weak to moderate activity was observed against the gram-positive strains *B. cereus* and *S. aureus*. The nature of the substituent on the benzene ring has no pronounced influence on the antimicrobial potency. Overall, compounds **1**–**3** exhibited antibacterial activity comparable to that of commercial benzalkonium chloride. Antifungal activity against *Candida* species was comparable to that of the naftifine hydrochloride. It was also noted in the literature that gram-positive bacteria were more sensitive to α-hydroxyphosphonate derivatives than gram-negative bacteria. Some of phosphonates also exhibited pronounced antifungal activity, which overall indicates the promise of the α-hydroxyphosphonate scaffold for the development of antimicrobial agents.[42–44]

In conclusion, we demonstrated a facile and environmentally friendly solvent-free synthesis of dipropyl α-hydroxy(aryl)-methylphosphonates *via* the Abramov reaction. The crystallographic analysis of the products revealed a one-dimensional chain formed by O–H···O hydrogen bonds as the primary supramolecular motif, while the nature of the substituent on the benzene ring dramatically influenced the higher-order crystal packing. Thermal decomposition behaviour, studied by TG-DSC, correlated with the electronic nature of the substituent on the benzene ring. All compounds displayed antibacterial activity against the gram-positive bacteria *B. cereus* and *S. aureus* comparable to that of benzalkonium chloride, as well as moderate fungicidal activity against *Candida* species. We hope this work provide a solid foundation for the design of readily accessible candidates for antimicrobial drugs based on α-hydroxy-alkylphosphonates.

Table 2 Antimicrobial activity of compounds **1**–**3**.

Compound	Diameter of growth inhibition zone *d*/mm[a]				
	Gram-negative		Gram-positive		Fungi
	E. coli	*Ps. aeruginosa*	*B. cereus*	*S. aureus*	*C. albicans*
1	7±1	7±1	19±2	10±1	11±1
2	8±1	7±1	19±2	10±1	11±1
3	7±1	7±1	15±2	10±1	11±1
Naftifine hydrochloride[b]	n/m[c]	n/m	n/m	n/m	12±1
Benzalkonium chloride	8±1	11±1	15±2	13±1	10±1

[a] Average of three values measured; ± standard deviation (SD); zone of inhibition 22 to 33: highly significant, between 15 to 21 mm: less significant, below 14 mm: poor activity. [b] Ethanol solution, 1% (Mycoderil). [c] Not measured.

«This work/publication was funded by a grant from the Academy of Sciences of the Republic of Tatarstan provided to higher education institutions, scientific and other organizations to support human resource development plans in terms of encouraging their research and academic staff to defend doctoral dissertations and conduct research activities (Agreement No. 12/2025-PD-KFU dated December 22, 2025)».

Online Supplementary Materials

Supplementary data associated with this article can be found in the online version at doi: 10.71267/mencom.8102.

References

1 Z. Radai and G. Keglevich, *Molecules*, 2018, **23**, 1493; https://doi.org/10.3390/molecules23061493.
2 N. Z. Kiss, Z. Radai and G. Keglevich, *Phosphorus, Sulfur Silicon Relat. Elem.*, 2019, **194**, 1003; https://doi.org/10.1080/10426507.2019.1630407.
3 C. Sampath, C. Naga Raju and C. Venkata Rao, *Phosphorus, Sulfur Silicon Relat. Elem.*, 2016, **191**, 95; https://doi.org/10.1080/10426507.2015.1032412.
4 H.-J. Hu, R.-L. Gao, Q.-F. Yang, Y.-P. Huang, H.-M. Wang and C.-X. Pei, *New J. Chem.*, 2022, **46**, 7987; https://doi.org/10.1039/d2nj00295g.
5 Y. R. Lima, G. P. Da Costa, M. C. D. Xavier, M. C. De Moraes, T. Barcellos, D. Alves and M. S. Silva, *ChemistrySelect*, 2020, **5**, 12487; https://doi.org/10.1002/slct.202003761.
6 R. R. Ummadi, V. N. Ratnakaram, S. R. Devineni, C. Subramanyam and C. M. Pavuluri, *Res. Chem. Intermed.*, 2025, **51**, 3767; https://doi.org/10.1007/s11164-025-05622-4.
7 B. Stowasser, K.-H. Budt, L. Jian-Qi, A. Peyman and D. Ruppert, *Tetrahedron Lett.*, 1992, **33**, 6625; https://doi.org/10.1016/S0040-4039(00)61002-X.
8 A. H. Kategaonkar, R. U. Pokalwar, S. S. Sonar, V. U. Gawali, B. B. Shingate and M. S. Shingare, *Eur. J. Med. Chem.*, 2010, **45**, 1128; https://doi.org/10.1016/j.ejmech.2009.12.013.
9 K. R. M. Naidu, K. S. Kumar, P. Arulselvan, C. B. Reddy and O. Lasekan, *Arch. Pharm.*, 2012, **345**, 957; https://doi.org/10.1002/ardp.201200192.
10 Z. Radai, P. Szeles, N. Z. Kiss, L. Hegedűs, T. Windt, V. Nagy and G. Keglevich, *Heteroat. Chem.*, 2018, **29**, e21436; https://doi.org/10.1002/hc.21436.
11 F. Mary, G. Arrachart, A. Leydier and S. Pellet-Rostaing, *Tetrahedron*, 2019, **75**, 3968; https://doi.org/10.1016/j.tet.2019.06.004.
12 M. Stankevic, J. Pisklak and K. Wlodarczyk, *Tetrahedron*, 2016, **72**, 810; https://doi.org/10.1016/j.tet.2015.12.043.
13 C. dos Santos, L. S. dos Santos and O. L. Franco, *J. Antibiot.*, 2021, **74**, 547; https://doi.org/10.1038/s41429-021-00444-z.
14 K.-S. Ju, J. R. Doroghazi and W. W. Metcalf, *J. Ind. Microbiol. Biotechnol.*, 2014, **41**, 345; https://doi.org/10.1007/s10295-013-1375-2.
15 E. I. Parkinson, A. Erb, A. C. Eliot, K.-S. Ju and W. W. Metcalf, *Nat. Chem. Biol.*, 2019, **15**, 1049; https://doi.org/10.1038/s41589-019-0343-1.
16 H. Jomaa, J. Wiesner, S. Sanderbrand, B. Altincicek, C. Weidemeyer, M. Hintz, I. Turbachova, M. Eberl, J. Zeidler, H. K. Lichtenthaler, D. Soldati and E. Beck, *Science*, 1999, **285**, 1573; https://doi.org/10.1126/science.285.5433.1573.
17 T. Knak, M. A. Abdullaziz, S. Höfmann, L. A. Alves Avelar, S. Klein, M. Martin, M. Fischer, N. Tanaka and T. Kurz, *Pharmaceuticals*, 2022, **15**, 1553; https://doi.org/10.3390/ph15121553.
18 L. A. Walker, V. Bagonza, B. Bobb and D. J. Sullivan, *Int. J. Parasitol.: Drugs Drug Resist.*, 2025, **27**, 100577; https://doi.org/10.1016/j.ijpddr.2024.100577.

19 P. G. Leonard, N. Satani, D. Maxwell, Y.-H. Lin, N. Hammoudi, Z. Peng F. Pisaneschi, T. M. Link, G. R Lee, IV, D. Sun, B. A. Bhanu Prasad, M. E. Di Francesco, B. Czako, J. M. Asara, Y. Alan Wang, W. Bornmann, R. A DePinho and F. L. Muller, *Nat. Chem. Biol.*, 2016, **12**, 1053; https://doi.org/10.1038/nchembio.2195.

20 F. Pisaneschi, Y.-H. Lin, P. G. Leonard, N. Satani, V. C. Yan, N. Hammoudi, S. Raghavan, T. M. Link, D. K. Georgiou, B. Czako and F. L. Muller, *Molecules*, 2019, **24**, 2510; https://doi.org/10.3390/molecules24132510.

21 J. Krucinska, M. N. Lombardo, H. Erlandsen, A. Hazeen, S. S. Duay, J. G. Pattis, V. L Robinson, E. R. May and D. L. Wright, *Sci. Rep.*, 2019, **9**, 17106; https://doi.org/10.1038/s41598-019-53301-3.

22 Y.-H. Lin, N. Satani, N. Hammoudi, V. C. Yan, Y. Barekatain, S. Khadka, J. J. Ackroyd, D. K. Georgiou, C.-D. Pham, K. Arthur, D. Maxwell, Z. Peng, P. G. Leonard, B. Czako, F. Pisaneschi, P. Mandal, Y. Sun, R. Zielinski, S. C. Pando, X. Wang, T. Tran, Q. Xu, Q. Wu, Y. Jiang, Z. Kang, J. M. Asara, W. Priebe, W. Bornmann, J. R. Marszalek, R. A. DePinho and F. L. Muller, *Nat. Metab.*, 2020, **2**, 1413; https://doi.org/10.1038/s42255-020-00313-3.

23 V. C. Yan, K. L. Yang, E. S. Ballato, S. Khadka, P. Shrestha, K. Arthur, D. K. Georgiou, M. Washington, T. Tran, A. H. Poral, C.-D. Pham, M. J. Yan and F. L. Muller, *ACS Med. Chem. Lett.*, 2020, **11**, 1484; https://doi.org/10.1021/acsmedchemlett.0c00203.

24 V. C. Yan, C. D. Pham, E. S. Ballato, K. L. Yang, K. Arthur, S. Khadka, Y. Barekatain, P. Shrestha, T. Tran, A. H. Poral, M. Washington, S. Raghavan, B. Czako, F. Pisaneschi, Y.-H. Lin, N. Satani, N. Hammoudi, J. J. Ackroyd, D. K. Georgiou, S. W. Millward and F. L. Muller, *J. Med. Chem.*, 2022, **65**, 13813; https://doi.org/10.1021/acs.jmedchem.2c01039.

25 V. C. Yan, Y. Barekatain, Y.-H. Lin, N. Satani, N. Hammoudi, K. Arthur, D. K. Georgiou, Y. Jiang, Y. Sun, J. R. Marszalek, S. W. Millward and F. L. Muller, *ACS Pharmacol. Transl. Sci.*, 2023, **6**, 245; https://doi.org/10.1021/acsptsci.2c00216.

26 J. E. Milanes, V. C. Yan, C.-D. Pham, F. Muller, S. Kwain, K. C. Rees, B. N. Dominy, D. C. Whitehead, S. W. Millward, M. Bolejack, R. Shek, L. Tillery, I. Q. Phan, B. Staker, E. Ashley Moseman, X. Zhang, X. Ma, A. Jebet, X. Yin and J. C. Morris, *PLoS Pathog.*, 2024, **20**, e1012412; https://doi.org/10.1371/journal.ppat.1012412.

27 C. P. Roster, D. LaVigne, J. E. Milanes, E. Knight, H. D. Anderson, S. Pizarro, E. M. Harding, M. T. Morris, V. C. Yan, C.-D. Pham, F. Muller, S. Kwain, K. C. Rees, B. Dominy, D. C. Whitehead, M. N. Uddin, S. W. Millward and J. C. Morris, *Pathogens*, 2023, **12**, 1290; https://doi.org/10.3390/pathogens12111290.

28 L. Ouksel, S. Chafaa, R. Bourzami, N. Hamdouni, M. Sebais and N. Chafai, *J. Mol. Struct.*, 2017, **1144**, 389; https://doi.org/10.1016/j.molstruc.2017.05.029.

29 I. Essid, S. Soudani, F. Lefebvre, W. Kaminsky, W. Fujita, C. B. Nasr and S. Touil, *J. Mol. Struct.*, 2017, **1149**, 99; https://doi.org/10.1016/j.molstruc.2017.07.074.

30 Z. Szalai, A. S. Kis, A. Takács, L. Köhidai, K. Karaghiosoff, M. Czugler, L. Drahos and G. Keglevich, *Molecules*, 2025, **30**, 428; https://doi.org/10.3390/molecules30020428.

31 Z. Radai, N. Z. Kiss, M. Czugler, K. Karaghiosoff and G. Keglevich, *Acta Crystallogr., Sect. C: Struct. Chem.*, 2019, **75**, 283; https://doi.org/10.1107/S2053229619001839.

32 R. Davletshin, A. Sedov, K. Ivshin, N. Davletshina, E. Sokolova, P. Zelenikhin, A. Baklagina, M. Shulaeva, A. Gerasimov and P. Kuryntseva, *J. Mol. Struct.*, 2025, **1353**, 144619; https://doi.org/10.1016/j.molstruc.2025.144619.

33 P. G. Mandhane, R. S. Joshi, D. R. Nagargoje and C. H. Gill, *Tetrahedron Lett.*, 2010, **51**, 1490; https://doi.org/10.1016/j.tetlet.2010.01.031.

34 R. R. Davletshin, A. N. Sedov, M. P. Shulaeva, K. A. Ivshin, N. V. Davletshina, A. V. Gerasimov, P. A. Kuryntseva and S. V. Mosunova, *Mendeleev Commun.*, 2025, **35**, 152; https://doi.org/10.71267/mencom.7587.

35 M. A. Kulkarni, U. P. Lad, U. V. Desai, S. D. Mitragotri and P. P. Wadgaonkar, *C. R. Chim.*, 2013, **16**, 148; https://doi.org/10.1016/j.crci.2012.10.009.

36 L. J. Bellamy, *The Infra-red Spectra of Complex Molecules*, Springer, Dordrecht, 1975; https://link.springer.com/book/10.1007/978-94-011-6017-9.

37 A. N. Sedov, R. R. Davletshin, N. V. Davletshina, K. A. Ivshin, A. P. Fedonin, A. R. Osogostok and M. P. Shulaeva, *Russ. J. Org. Chem.*, 2023, **59**, 1342; https://doi.org/10.1134/S1070428023080080.

38 R. R. Davletshin, A. N. Sedov, N. V. Davletshina, K. A. Ivshin, A. P. Fedonin, A. R. Osogostok and R. A. Cherkasov, *Russ. J. Phys. Chem. A*, 2023, **97**, 1402; https://doi.org/10.1134/S0036024423070063.

39 L. Ouksel, R. Bourzami, N. Hamdouni and A. Boudjada, *J. Mol. Struct.*, 2021, **1229**, 129792; https://doi.org/10.1016/j.molstruc.2020.129792.

40 L. Zhou, G. Zhang, J. Li, Z. Jing, J. Qin and Y. Feng, *J. Therm. Anal. Calorim.*, 2017, **129**, 1667; https://doi.org/10.1007/s10973-017-6319-z.

41 M. A. de Sousa Rios and S. E. Mazzeto, *Fuel Process. Technol.*, 2012, **96**, 1; https://doi.org/10.1016/j.fuproc.2011.12.004.

42 J. R. Telu, N. Kuntala, K. Kankanala, V. Bonothu, R. Kapavarapu, S. Pal and J. S. Anireddy, *J. Mol. Struct.*, 2025, **1344**, 142816; https://doi.org/10.1016/j.molstruc.2025.142816.

43 A. H. Kategaonkar, R. U. Pokalwar, S. S. Sonar, V. U. Gawali, B. B. Shingate and M. S. Shingare, *Eur. J. Med. Chem.*, 2010, **45**, 1128; https://doi.org/10.1016/j.ejmech.2009.12.013.

44 R. U. Pokalwar, R. V. Hangarge, P. V. Maske and S. V. Shinde, *Arkivoc*, 2006, 196; https://doi.org/10.3998/ark.5550190.0007.b20.

Received: 25th May 2026; Com. 26/8102

Contents entry

Molecular structure, thermal, and antimicrobial properties of dipropyl [hydroxy(aryl)methyl]-phosphonates

Rustam R. Davletshin, Andrey N. Sedov, Kamil A. Ivshin, Marina P. Shulaeva, Alexander V. Gerasimov, Natal'ya V. Davletshina, Timofey T. Senchenko, Polina A. Kuryntseva

